Accepted Manuscript

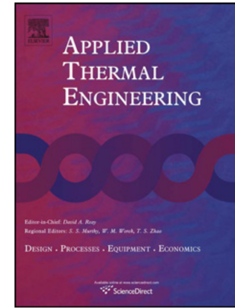

A Liquid-Based System for CPU Cooling Implementing a Jet Array Impingement Waterblock and a Tube Array Remote Heat Exchanger

B.P. Whelan, R.S. Kempers, A.J. Robinson

PII: S1359-4311(12)00015-4

DOI: 10.1016/j.applthermaleng.2012.01.013

Reference: ATE 3962

To appear in: *Applied Thermal Engineering*

Received Date: 7 February 2011

Revised Date: 22 December 2011

Accepted Date: 5 January 2012

Please cite this article as: B.P. Whelan, R.S. Kempers, A.J. Robinson, A Liquid-Based System for CPU Cooling Implementing a Jet Array Impingement Waterblock and a Tube Array Remote Heat Exchanger, *Applied Thermal Engineering* (2012), doi: 10.1016/j.applthermaleng.2012.01.013

This is a PDF file of an unedited manuscript that has been accepted for publication. As a service to our customers we are providing this early version of the manuscript. The manuscript will undergo copyediting, typesetting, and review of the resulting proof before it is published in its final form. Please note that during the production process errors may be discovered which could affect the content, and all legal disclaimers that apply to the journal pertain.

ACCEPTED MANUSCRIPT

A Liquid-Based System for CPU Cooling Implementing a Jet Array Impingement Waterblock and a Tube Array Remote Heat Exchanger

B.P. Whelan[1], R.S. Kempers[1,2], A.J. Robinson[1,*]
[1]Department of Mechanical and Manufacturing Engineering, Trinity College Dublin, Ireland
[2]Alcatel-Lucent, Blanchardstown, Ireland

[*]Corresponding author. Tel: +353 1 8963919
E-mail addresses: arobins@tcd.ie (A.J. Robinson)

ACCEPTED MANUSCRIPT

ACCEPTED MANUSCRIPT

A Liquid-Based System for CPU Cooling Implementing a Jet Array Impingement Waterblock and a Tube Array Remote Heat Exchanger

B.P. Whelan[1], R.S. Kempers[1,2], A.J. Robinson[1]
[1]Department of Mechanical and Manufacturing Engineering, Trinity College Dublin, Ireland
[2]Alcatel-Lucent, Blanchardstown, Ireland

ABSTRACT

A liquid CPU cooler has been designed and tested with the aim to achieve a cooling capacity of 200 W for a surface area of 8.24 cm^2, commensurate with the integrated heat spreader dimensions of an Intel® Pentium® 4 Processor. The primary aim of the design was to develop thermal hardware components that can be manufactured simply and cost effectively. To this end, a miniature jet array waterblock and a tube bundle remote heat exchanger were employed since the bulk of their housings could be manufactured using low cost injection molding techniques which could significantly reduce the total system cost compared with conventional units. The system was capable of dissipating the required heat load and exhibited an overall thermal resistance of 0.18 K/W requiring approximately 1.5 W of hydraulic power. At maximum power the chip-to-air temperature difference was 45°C which is adequately close to typical design thresholds. The influences of power loading and liquid volumetric flow rate are also discussed.

KEYWORDS:
Electronics Cooling, Liquid Jet Impingement, CPU Thermal Management, Waterblock

ACCEPTED MANUSCRIPT

1. INTRODUCTION

During operation all electronic devices generate heat that must be dissipated effectively in order to ensure proper functioning and reduce the risk of failure. In devices such as microprocessors, temperature thresholds (typically ~85°C at present) are imposed to reduce leakage currents. From a reliability standpoint, elevated temperatures and cyclic temperature excursions can induce failure mechanisms which will cause premature component failure [1]. The proper functioning and reliability of electronic components hinges on adequate thermal management. However, advances in micro-fabrication of electronic circuitry have lead to continual decreases in dimensions ostensibly allowing more circuit components per unit surface area. This has lead to severe increases in power densities and have strained existing air based board level thermal management hardware, such as the low-tech fan-finned heat sink, to their operational limits.

It is accepted that chip heat fluxes will continue to escalate in the coming years. Current fan-fin cooling techniques will not be a viable solution at board level primarily due to fin efficiency and heat spreading bottlenecks and the fact that air is a poor thermal transport medium. One of the main conundrums is that the heat transfer coefficient generally increases asymptotically with air velocity ($h \alpha u^{0.8}$) whereas the pressure drop penalty increases as $\Delta P \alpha u^2$ and acoustic noise at somewhere in the region of $U \alpha u^5$. This being the case there are very disproportionately large increases in penalties with modest gains in heat transfer.

Liquid based cooling of electronics is an obvious choice due to their superior thermophysical properties compared with air. Liquid based heat sinks extract the heat with very reduced form factors at board level since the heat is released to the air by a remote heat sink, typically where there is sufficient real estate that form factor constraints are not as severe. Furthermore, the liquid flow in the remote heat exchanger precludes the need for advanced heat spreading technologies.

Over the past 20 years there has been very aggressive international research effort regarding single and two-phase microchannels [2, 3]. Single-phase channel flow affords reasonable heat transfer coefficients whilst offering the enticing possibility of a very high heat transfer surface areas per unit volume. One drawback, however, is the singular direction of the flow which can result in large temperature gradients from inlet to outlet which are undesirable

ACCEPTED MANUSCRIPT

ACCEPTED MANUSCRIPT

[4]. A possible solution to this is two-phase convective flow which should ideally be more isothermal. However, two-phase flow in microchannels has proven to be extremely complex, both with regards to the overall heat transfer coefficient and the dryout limit [3], and it is not likely that a reliable and affordable two phase heat sink will be available in the near future.

The preponderance of commercially available board level liquid cooling technologies for electronics thermal management, termed waterblocks, generally implement small scale surface extensions to increase the surface area for heat transfer for low effective liquid velocities and consequent heat transfer coefficients. The drawback of this approach, similarly to the microchannel approach, is that the heat sinks require micro-manufacturing of the small features, typically on copper, which adversely adds to the overall cost of the waterblock making them far from cost competitive compared with simple extruded aluminum heat sinks. Further to this, the heat must ultimately be released to ambient air by a remote heat sink which further adds to the overall system cost.

Recently there has been some work done which addresses the total system thermal resistance of liquid cooling systems including the remote heat exchanger. Bintoro et al. [5] developed a direct contact single water jet impingement device combined with a minichannel remote heat exchanger for CPU cooling. The cooling system maintained the chip's surface temperature to just below 95 °C at the maximum heat load of 200 W. Assuming an ambient temperature of 20°C, the overall chip to air thermal resistance was in the range of 0.35 K/W. Liu et al. [6] utilized a microjet array with mini fan cooled remote heat exchanger for cooling high power LEDs and achieved an overall thermal resistance of about 0.17 K/W. Chang et al. [7] were able to achieve an overall thermal resistance of 0.23 K/W by implementing a microchannel heat sink in conjunction with a plate-fin type remote heat exchanger of which just under half (43%) was due to the microchannel heat sink.

The objective of the present study is to develop and test a closed loop liquid cooling system for a commercially available CPU that adequately dissipates a load of 200 W with heat sinks that can be manufactured inexpensively. To this end it was decided to focus on heat sink housings that are amenable to injection molded plastic while at the same time reducing the overall metal content and other cost intensive manufacturing processes such as micromachining.

ACCEPTED MANUSCRIPT

2. EXPERIMENTAL APPARATUS

2.1 Heater Block

The heater block and housing used in this study is shown schematically in Fig. 1 and were designed to emulate that of an Intel Pentium 4 processor, equipped with an Integrated Heat Spreader (IHS), attached to a LGA-775 package. The Intel® Pentium® 4 Processor thermal design guide data sheet [8] provided the dimensions implemented in the heater block and housing design. A square surface of 28.7 x 28.7 mm, equivalent to that of the top surface of the IHS, was used as the heater surface. A 72 x 72 mm square array of 4 threaded holes was centred at the copper block. The threaded holes are used to attach the water block to the heater block housing.

In order to determine the temperature distribution and the heat flux, three thermocouples were embedded at known locations along the heater block. Due to its high thermal conductivity copper was chosen as the heater block material. In order to provide sufficient power to the exposed surface, two cartridge heaters of 6.25 mm diameter and 46 mm length, each with a power rating of 175 W, were utilized. Nylon was chosen as the housing material as it possesses a relatively high melting point as well as a low thermal conductivity which reduces losses. Fig. 1 depicts the final heater block assembly.

2.2 Flow delivery and monitoring system

The experimental apparatus used in the testing procedure consisted of a water delivery and monitoring system, as well as the previously described heater block and housing. A schematic of the arrangement used in the experiment is depicted in Fig. 2. The arrangement sought to mimic that of a commercial closed water loop used in the cooling of a CPU, and therefore popular commercial components were used when possible.

The flow loop consisted of a pump which drew deionized water from a 1.5 L water reservoir manufactured by Danger Den (Astoria, Oregon). The pump used in the system was the Laing DD12V-D5 Variable Speed Pump. This pump contained five different settings that were used to control the flow rate through the system. The power delivered to the pump was controlled using a Lascar PSU 130 adjustable DC power supply. In order to monitor the flow rate, a rotameter, with a flow range of 2-10 LPM ± 1.5% FS, was installed within the system. T-type sheathed thermocouples of 1.5 mm diameter were used in conjunction with Fluke54II Thermometers

ACCEPTED MANUSCRIPT

(±0.3°C), to measure and record the water temperatures at the inlet and outlet of the water block as well as the outlet of the heat exchanger. Pressure taps were also installed on either side of the water block and heat exchanger and measurements were obtained using two Digitron 2083P (0-2 bar ± {0.1% rdg + 0.1% FS}) differential pressure meters. In order to determine the outlet temperature of the air after passing through the heat exchanger, a K-type thermocouple was positioned in nine different locations, with the average of the readings utilized as the effective air exit temperature. The power delivered to the fan was also controlled by a Lascar PSU 130 adjustable DC power supply. The radiator was coupled with an EMB Papst 5912-3214JH3 fan, which could provide a maximum air flow rate of 140 CFM. Hot wire measurements indicated that this corresponded with an air velocity of about 4.5 m/s.

A layer of Thermal Interface Material (Arctic Silver 5) was applied between the heated surface and the waterblock. As a result of the thermal resistance of this layer the surface temperature of the heater block would be higher than that of the base of the water block. Therefore, a fine wire thermocouple was fastened to the base of the waterblock and this temperature was used in calculation of various performance indicators.

2.3 Data Reduction

The heat flux, $Q^{//}$, at the heater surface was assumed to be uniform and was calculated from,

$$Q^{//} = -k_{Cu} \left. \frac{dT}{dz} \right|_{\substack{best \\ fit}} \quad (1)$$

where k_{cu} is the thermal conductivity of the copper, evaluated at the average block temperature, and $dT/dz|_{best\ fit}$ is the linear regression fit of the centreline temperature measurement. The power delivered by the heated surface to the water block is determined from the expression,

$$Q = Q^{//} A_s \quad (2)$$

The thermal resistances, R_{th}, of both the waterblock and heat exchanger were determined using the equation,

$$R_{th} = \frac{\Delta T_{lm}}{Q} \quad (3)$$

The use of the log-mean temperature difference has been selected for the analysis of both the waterblock and the remote liquid-to-air remote heat exchanger for consistency. For the

ACCEPTED MANUSCRIPT

waterblock, the difference between the wall and inlet water temperatures could have been chosen as in Iyenger et al. [9]. However, since the temperature drop across the water block was generally ~1°C the two methods give nearly identical results.

The log mean temperature difference across the water block is defined as,

$$\Delta T_{lm_Wb} = \frac{(T_{wb} - T_{out}) - (T_{wb} - T_{in})}{\ln\left[(T_{wb} - T_{out}) / (T_{wb} - T_{in}) \right]} \qquad (4)$$

Here, T_{wb} is the temperature at the bottom of the water block, T_{in} is the inlet temperature and T_{out} is the outlet temperature. The log mean temperature difference across the air cooled heat exchanger is defined as,

$$\Delta T_{lm_Hx} = \frac{(T_{Hx_in} - T_{A_out}) - (T_{Hx_out} - T_{\infty})}{\ln\left[(T_{Hx_in} - T_{A_out}) / (T_{Hx_out} - T_{\infty}) \right]} \qquad (5)$$

where T_{W_in} is the inlet water temperature, T_{W_out} is the outlet water temperature, T_{∞} is the ambient temperature which was used as the inlet air temperature and T_{A_out} is the outlet air temperature.

The uncertainty on derived quantities are listed in Table I for the lowest and highest nominal power settings and the highest flow rate tested. Of particular note is that the Monte Carlo method developed by Kempers *et al* [10] was used to determine the uncertainty on the heat flux based on Eq. 1, which was subsequently incorporated into the uncertainty of the power and thermal resistance values. As it is detailed, the uncertainty in the imposed power, and subsequent thermal resistance values, are in the range of 20% at the lowest heat load and decrease to 6% at the highest heat load. The pumping power uncertainty is generally about 5% which is acceptable.

Table I: Uncertainty of derived quantities for nominal power settings of 50W and 200W for a volumetric flow rate of 5.25 LPM.

Q		**$R_{th,wb}$ (jets)**		**R_{th} (tubes)**		**Q_{pump}**	
50W	**200W**	**50W**	**200W**	**50W**	**200W**	**50W**	**200W**
± 18%	± 6%	±20%	± 6%	±21%	±6%	±5%	± 5%

ACCEPTED MANUSCRIPT

3. HEAT EXCHANGER DESIGNS

3.1 Waterblock Design

A primary goal of this work is to design a high performance waterblock of which the majority of the structure being amenable to very low cost injection molding, reduced volume of metal and minimal, if any, complex machining. To this end microchannels and mini/macro surface extensions were ruled out and a liquid jet array waterblock was conceived and is illustrated in Fig. 3. Impinging liquid jets afford a very high single phase heat transfer coefficient such that thermal resistances comparable or exceeding microchannels or micro-featured surfaces can be obtained without surface modification. Also, as it is shown in the Fig. 3, the primary housing can be constructed from plastic. For this work the housing was fabricated from VisiJet® SR200 - UV curable acrylic plastic rapid prototyped on a 3D Systems InVision 3D printer.

The target cooling capacity was 200 W which corresponds with a heat flux of 243 kW/m^2. A thermal resistance of R_{th} =0.075 K/W was selected which results in a target surface to inlet coolant temperature difference of 15°C. This resistance has two constituents, one accounting for the resistance of the copper base which is R_{Cu} = 0.01 K/W and the other associated with the heat transfer to the liquid stream, which must be R_{jets} = 0.065 K/W in order to achieve the design point thermal resistance.

The liquid jet array waterblock design is illustrated in Fig. 3. Water enters into a plenum chamber and passes through the array of jets and onto the copper base. The upper impingement surface is 27.5 mm x 27.5 mm and is stepped up to 28.7 mm x 28.7 mm at the base. Although it is known to be deleterious with regards to the heat transfer, it was decided to confine the flow to exit at only one end of the lower channel. This simplified the internal structure of the device such that injection moulding would be feasible. It also allows for a lower profile compared with one with four exit streams that would have to be then be recombined in a second upper plenum. This last point is crucial in the design of thermal management hardware as there are strict limitations on the allowable size of devices, particularly at board level. One reason for this is that larger devices generally offer excessive pressure drop of the circulating air which adversely affects the cooling of downstream components.

Compared with its microchannel counterpart, there are far fewer correlations for jet array impingement heat transfer, though some exist [11-17]. For this work, the Robinson-Schnitzler

correlations [17] have been used because they were developed for submerged jets, consider the influence of jet to target confinement and inter jet spacing and provide information about the friction factor. Robinson and Schnitzler correlated their average heat transfer data for confined-submerged jets as:

$$Nu_d = 1.485\,\mathrm{Re}_d^{0.46}\left(\frac{S}{d}\right)^{-0.442}\left(\frac{H}{d}\right)^{-0.00716}\mathrm{Pr}^{0.4} \qquad (6)$$

The correlation was found to agree very well with the correlation of Womac et al [16]. Further to this, the friction factor for both free and submerged jet arrays was correlated as:

$$f = 0.51 + \frac{229.9}{\mathrm{Re}_d} \qquad (7)$$

Eq. 7 was found to be in close agreement with that of Fabbri and Dhir [11] albeit the latter work was performed for the impingement of free surface microjets. Recently, Whelan and Robinson [18] showed that the pressure drop penalty could be notably reduced by chamfering the orifice inlet without significantly affecting the heat transfer.

Eqs. 6 and 7 were used to obtain the flow rates, geometrical layout and corresponding pressure drops that can achieve the required surface average heat transfer coefficient. Based on the target jet array thermal resistance and impingement surface area, a heat transfer coefficient of approximately h_{jets}=20,000 W/m^{2}K is required. However, the Robinson-Schnitzler correlation was developed for minimal confinement and would be expected to over predict the heat transfer coefficient. A study on the influence of crossflow was performed by Obot and Trabold [19]. They demonstrated that for air jet arrays, degradation in heat transfer of up to a factor of two can occur when the impingement surface is confined on three of its sides which has been accounted for in the present calculations.

In order to obtain the heat transfer coefficient from the Robinson-Schnitzler correlation, the number of jets that could impinge onto the square copper surface was calculated using the expression similar to that developed by Robinson [20],

$$N_{Total} = \left(\frac{\left(L_S - \{S + d_n\}\right)}{S} + 2\right)^2 \qquad (8)$$

where L_S is the length of one side of the impingement surface, in this case 27.5 mm, S is the interjet spacing and d_n is the jet nozzle diameter which was kept at 1.0 mm. This was applied for

ACCEPTED MANUSCRIPT

interjet spacing in the range of $2 \leq S/d_n \leq 6$,a nozzle exit-to-target spacing of $H/d_n = 3$ over a volumetric flow rate range of $0.5 \leq \dot{V} \leq 10$ L/min.

A limiting factor on the design was the pressure head available from the pump. The pressure head varied from 40 kPa to 24 kPa as the volumetric flow rate increased from 0 – 10 L/min. Also, the pump must supply adequate pressure head to accommodate the pressure drop associated with all of the other system components, including the remote heat sink, so that pressure drop across the waterblock must be considerably less than pressure head available.

Upon varying the interjet spacing and flow rate it was estimated that 49 individual 1 mm jets at an interjet spacing of $S/d_n = 4$ would achieve the required heat transfer coefficient at a flow rate of 6.5 L:min and a pressure drop of 6.54 kPa across the orifice plate. Accounting for other minor losses such as the expansion into the plenum, friction within the lower channel and a sudden contraction at the exit increases the predicted pressure drop of the waterblock assembly to 10.14 kPa.

3.2 *Remote Heat Exchanger Design*

As with the waterblock design, the motivation here is to design the remote heat exchanger to meet the thermal performance target with minimal size whilst having a great deal of its components compatible with low cost injection molding manufacturing. Since plastics have a low thermal conductivity it is not feasible to use them as the heat transfer surface material, which must be metallic. Based on this the device illustrated in Fig. 4 was conceived. The heat exchanger consists of two plastic inlet and outlet plenums and a tube bundle in cross flow with air over its outer surface and hot water flowing on the inside of the tubes. Based on a set of constraints that will be outlined below, the remote heat exchanger cooling capacity design point was 200 W without excessive pressure drop on both the air and water sides.

Predicting the heat transfer rate from a tube bundle heat exchanger depends on numerous parameters including the approaching air velocity, U_{app}, coolant volumetric flow rate, $\dot{V}$, number of tubes, N_{Tubes}, tube-to-tube spacing in both the transverse and longitudinal directions, S_T & S_L, tube inner diameter, $d_{tube,i}$, tube wall thickness, t_{tube}, ambient air temperature T_∞, and the water temperature at the inlet, T_{Hx_in}.

ACCEPTED MANUSCRIPT

In the design of this heat exchanger the number of variables was reduced by fixing certain parameters and defining reasonable constraints. Pressure drop on the water side was targeted to be less than 7 kPa, as it had to be within the limitations of the system's pumping capabilities considering that the waterblock consumes approximately half of that available from the pump. Also, pressure drop on the air side had to be kept below a reasonable limit, which would be dependent on the capabilities of the selected fan, as will be discussed. Furthermore, a limitation on the incoming air velocity needed to be established. A survey of commercial fans indicated that air speeds above 5 m/s are sparse, and hence this value was selected as the air speed threshold in the design calculations. Also, due to the generally higher overall heat transfer coefficients compared with in line tube bundle, only the staggered arrangement was investigated with $S_T = S_L$. With regards to the heat exchanger dimension its length and width was fixed at 92 mm x 92 mm commensurate with the fan dimensions. Based on a survey of commercially available small metallic tubing, the range of inner/outer diameters ranged between 0.794mm/1.588mm and 3.969mm/4.763mm and considering possible cost and weight implications only aluminum was considered. Furthermore, finned tubes were not considered as it was thought that this would adversely affect cost. Based on the waterblock, analysis the water flow rate was fixed at 6.5 L/min. While conforming to all of these design constraints, it was aimed to dissipate the required heat load at the lowest possible overall heat exchanger volume.

The configuration for the staggered tube bundle arrangement is illustrated in Fig. 5. The total heat transfer rate, Q, from a tube bundle is dependent upon the number of tubes, N, the overall heat transfer coefficient, U, and the log mean temperature difference, ΔT_{lm}, and it is expressed as follows,

$$Q = NUA_o \Delta T_{lm} \qquad (9)$$

where

$$UA_o = \frac{1}{h_i A_i} + \frac{\ln(D_o / D_i)}{2\pi kL} + \frac{1}{h_o A_o} \qquad (10)$$

The log mean temperature difference was defined in Eq. 5.

For a single tube, the internal heat transfer coefficient, h_1, was determined by assuming fully developed laminar flow and constant surface temperature such that,

$$Nu_{Di} = \frac{h_i D_i}{k} = 3.66 \quad (11)$$

In order to determine the outer heat transfer coefficient for the tube bundle, the methodology of Khan et al. [22] was employed. In their study, Khan et al. [22] investigated heat transfer from tube banks in crossflow under isothermal boundary conditions. A Nusselt number correlation was provided as follows,

$$Nu_{Do} = \frac{h_o D_o}{k} = C_1 Re_{Do}^{1/2} Pr^{1/3} \quad (12)$$

Using this correlation, the outer heat transfer coefficient was determined. The coefficient C_1 is dependent on both the transverse, S_T, and longitudinal, S_L, tube-to-tube spacing and was found using the following,

$$C_1 = \frac{0.61 S_T^{0.091} S_L^{0.053}}{[1 - 2\exp(-1.09 S_L)]} \quad (13)$$

where,

$$S_L = S_L / D_o \quad \& \quad S_T = S_T / D_o \quad (14)$$

The Reynolds number was determined using,

$$Re_{d_{tube_o}} = \frac{D_o U_{max}}{\nu} \quad (15)$$

Due to the staggered nature of the tube bundles, different air velocities will exist as it flows through the bundle, due to contractions and expansions in the area through which it flows. U_{max} is the greatest air velocity that occurs within the bundle and is determined with the expression,

$$U_{max} = \max\left(\frac{S_T}{S_T - 1} U_{app}, \frac{S_T}{S_D - 1} U_{app}\right) \quad (16)$$

where S_D is defined as,

$$S_D = \sqrt{S_L^2 + \left(S_T / 2\right)^2} \quad (17)$$

As mentioned previously, pumping limitations impose a limit on the maximum permissible pressure drop that could occur across the water side of the heat exchanger. In initial calculations, only the pressure drop through the tubes was considered. Laminar flow was assumed and the pressure drop was calculated using,

ACCEPTED MANUSCRIPT

$$\Delta P = \frac{32 L u_{tube}^{2} \rho}{Re_{D_i} D_i} + 1.5\left(\frac{\rho u_{tube}^{2}}{2}\right) + 1.5\left(\frac{\rho U_o^2}{2}\right) \qquad (18)$$

where L is the tube length and u_{tube} is the mean water velocity in the tube and U_o is the liquid velocity entering and exiting the plenums. The first term in Eq.18 determines the pressure losses due to friction within the tube. The second term determines the losses associated with entry and exit to and from the tube. With regards to fan selection, the pressure drop on the air side is also important and was calculated from,

$$\Delta P = N_L \lambda \left(\frac{\rho U_{max}^2}{2}\right) f \qquad (19)$$

where N_L is the number of tubes in the longitudinal direction, which is the direction in which the air is flowing. The correction, λ, and friction, *f*, factors depend on the Reynolds number and the tube-to-tube spacing. The values for these parameters are presented in [21]. Also, all water properties were evaluated at the average water temperature, T_{surf_avg} and air properties were evaluated at the air side film temperature

Somewhat similar to the procedure outlined above for the waterblock, appropriate tube size, pitch and air velocity were specified. It was then determined how many tubes could fit vertically in each successive row and the number of rows increased until the required power was dissipated. This was done for inter tube spacing of $1.25 \leq S/d \leq 1.75$ and air velocities between 2 m/s and 5 m/s. Based on the predictions, it was estimated that a total of 90 tubes of D_o=3.969 mm and D_i=3.175 mm with a spacing of S/d=1.5 could dissipate the thermal load with a small enough pressure drop on both the liquid and air sides.

4. RESULTS AND DISCUSSION

3.1 Waterblock Only

Figure 6 illustrates the relationship between the thermal resistance and volumetric flow rate for the jet array waterblock as well as a popular commercially available waterblock (Danger Den MC-TDX CPU Cooler) for power loads of 100 W, 150 W and 200 W. Also shown in the figure is the predicted thermal resistance for the 200 W loading test. These tests were conducted using mains water supply with a nominal inlet temperature of 15°C to replicate the scenario of data centre cooling where the spent flow could be routed to a secondary chilling unit.

As evident from Fig. 6, the thermal resistance decreases with increases in volumetric flow rate for both units. Furthermore, the jets water block demonstrates a considerably better performance than the MC-TDX with thermal resistances, on average, 60% lower. The jets water block achieves its best performance at 10 L/min with a thermal resistance of R_{th} = 0.076 K/W, while similarly the MC-TDX achieves its best results with a thermal resistance of R_{th} = 0.149 K/W at the same flow rate. The predicted thermal resistance are consistently lower than the measured values though within 10-20% which can be considered adequate.

As mentioned previously, the pressure drop and hydraulic power requirements play important roles in a water block's suitability for implementation in the cooling of a CPU. Fig. 7 illustrates the corresponding relationships between the volumetric flow rate and pressure drop across each water block. Variations in pressure drop were found to be negligible at the different heater block power outputs. Furthermore, the predicted pressure drop across the waterblock is also included in the figure. As is evident the jets waterblock experiences pressure drop considerably greater than MC-TDX. Furthermore, the actual pressure drops across the jets water block exceed the predicted values by up to 19% in the upper flow rate ranges. This is reasonable considering the Robinson-Schnitzler correlation for the friction factor was developed with ±25% scatter bounds. Fig. 8 depicts the relationship between thermal resistance and pumping power for the jets and MC-TDX water blocks. As can be seen, the jets water block performs considerably better as a result of its superior heat transfer coefficient.

3.1 Waterblock and Remote Heat Exchanger Circuit

Figure 9 depicts the relationship between thermal resistance and power loading for both the jets water block and tube bundle heat exchanger at a flow rate of 5.25 L/min, which was the maximum achievable flow rate for the current set up. This is less than the desired flow rate of 6.5 L/min due to the pressure drop associated with the rotameter. Also included in the figure is the total thermal resistance of the system defined here as,

$$R_{th_System} = \frac{T_{WB} - T_{\infty}}{Q} \qquad (20)$$

The thermal resistance of the cooling system was found to decrease from about 0.25 K/W at 50 W and plateau approximately 0.18 K/W approaching 200 W. The increase is due to the increase in the average and film temperatures of the fluids which tends to increase thermal

conductivity and decrease viscosity in such a way as to improve the heat transfer coefficient. This is more marked for the remote heat exchanger which decreases by a factor of 1.9 between 50W and 200W which is a desirable trait for thermal management hardware. It should be noted that the predicted thermal resistance for an air speed of 4.5 m/s at 200 W was 0.044 K/W which compares favourably with the measured value 0.057 K/W, representing a 23% difference. It is suspected that a portion of this discrepancy can be accounted for by the poor distribution in the air velocity from the fan.

Figure 10 shows the variation of water inlet, waterblock base and the heater block surface temperature with imposed power. The heater block surface temperature of course depends on the thickness and effective thermal conductivity of the TIM layer. For this investigation an even layer of Arctic Silver 5 thermal paste was applied and 50 µm shim stock was used to level and fix the thickness of the TIM. It is evident from Fig. 10 that the cooling system is capable of maintaining a chip temperature of 65°C with a power loading of 200 W, which is a safe margin below the maximum operating temperature, generally quoted as 85°C. With a higher performance TIM the chip temperature would approach the waterblock base temperature which was 53°C at the highest power level.

Figure 11 depicts the relationships between thermal resistance and the liquid volumetric flow rate for a fixed heat load of 75 W. Also included in the figure is the relationship between the thermal resistance of the system and the volumetric flow rate. Both the water block and the remote heat exchanger thermal resistances decrease with increased volumetric flow rate. The compound effect is a steeper drop in the system thermal resistance.

Figure 12 shows the relationships between pumping power and volumetric flow rate, and the thermal resistance and pumping power for both the jets water block and tubes heat exchanger. The predicted pumping power values for the tube bundle and jets water block are also included in the figure. Fig. 12a shows that the predicted pumping power profiles compare reasonably well with the measured ones with the waterblock having the highest hydraulic power penalty. Fig. 12b shows that a system thermal resistance in the range of 0.2 K/W is achievable with a hydraulic power penalty of about 1.5 W.

ACCEPTED MANUSCRIPT

CONCLUSIONS

A liquid cooling system for CPU thermal management has been designed and tested for a cooling capacity of 200 W. A miniature jet array waterblock and a tube bundle remote heat exchanger were utilized since they could be manufactured using low cost injection molding which could significantly reduce the cost of the integrated system. The waterblock was designed to have as small as feasible footprint at board level whilst the remote heat sink was designed to dissipate the required heat load with as small a volume as possible under a pressure drop constraint.

The liquid based cooling system concept successfully dissipated the required 200 W with a chip temperature of 65°C and a waterblock base temperature of 53°C. The overall system thermal resistance was determined to decrease from 0.25 K/W at 50 W loading to 0.18 K/W at 200 W loading. A similar drop in the system thermal resistance was obtained for increasing the liquid volumetric flow rate between 2 L/min and 5.5 L/min.

Future work will address the thermal resistance of the waterblock. By unconfining the flow and adding a larger number of smaller diameter orifices it should be possible to significantly reduce thermal resistance and pressure drop thus that of the overall system.

ACKNOWLEDGMENTS

This work was supported by the CTVR, a CSET of Science Foundation Ireland. Particular gratitude is extended to Alcatel-Lucent Ireland.

ACCEPTED MANUSCRIPT

ACCEPTED MANUSCRIPT

NOMENCLATURE

A	area	[m^2]
C_p	specific heat capacity	[J/kgK]
d	diameter	[m]
D_i	tube internal diameter	[m]
D_o	tube outer diameter	[m]
f	friction factor	[-]
FS	Full Scale	[-]
g	gravity	[m/s^2]
h	convective heat transfer coefficient	[W/m^2K]
H	nozzle-to-target spacing	[m]
k	thermal conductivity	[W/mK]
L	length	[m]
$\dot{m}$	mass flow rate	[kg/s]
N	number of jets; number of tubes	[-]
Nu	Nusselt Number	[-]
ΔP	pressure drop	[Pa]
Pr	Prandtl number	[-]
Q	power	[W]
$Q^{//}$	heat flux	[W/m^2]
S	jet-to-jet spacing; tube-to-tube spacing	[m]
S_D	equation constant	[-]
S	spacing	[m]
r	radius	[m]
Re	Reynolds number	[-]
R_{th}	thermal resistance	[K/W]
t_n	nozzle plate thickness	[m]
T	temperature	[K]
U	overall heat transfer coefficient	[W/m^2K]

ACCEPTED MANUSCRIPT

U_o	liquid velocity in tube	[m/s]
u_{tube}	mean water	[m/s]
v	velocity	[m/s]
V_n	jet velocity	[m/s]
$\dot{V}$	volumetric flow rate	[m^3/s]
z	axial coordinate	[m]

Greek

α	thermal diffusivity	[m^2/s]
δ	boundary layer thickness	[m]
λ	correction factor	[-]
ρ	density	[kg/m^3]
σ	surface tension	[N/m]
μ	dynamic viscosity	[kg/ms]
ν	kinematic viscosity	[m^2/s]

Subscripts

cu	copper
f	fluid
film	film
h	hydrodynamic
hyd	hydraulic
Hx	heat exchanger
n	nozzle
o	stagnation point
out	out
s	surface
t	top
th	thermal
wb	water block

ACCEPTED MANUSCRIPT

REFERENCES

[1] P. Lall, M. Pecht, E. Hakim, "Influence of temperature on microelectronics and system reliability", CRC Press, New York., 1997, Ch 1.

[2] G.L. Morini, "Single-phase convective heat transfer in microchannels: a review of experimental results," Int. J. Thermal Sci., 43 (2004) 631-651.

[3] S. G. Kandlikar, High Flux Heat Removal with Microchannels: A Roadmap of Challenges and Opportunities," Heat Transfer Engineering, 26 (8) (2005) 5-14.

[4] J. Barrau, D. Chemisana, J. Rosell, L. Tadrist, M. Ibañez, An experimental study of a new hybrid jet impingement/micro-channel cooling scheme, Applied Thermal Engineering, 30 (2010) 2058-2066.

[5] J.S. Bintoro , A. Akbarzadeh, M. Mochizuki c," A closed-loop electronics cooling by implementing single phase impinging jet and mini channels heat exchanger," Applied Thermal Engineering 25 (2005) 2740–2753.

[6] S.Liu, J. Yang, Z. Gan,X. Luo," Structural optimization of a microjet based cooling system for high power LEDs," Int. J. Thermal Sci., 47 (8) (2008) 1086-1095.

[7] J.Y. Chang, H.S. Park, J. I. Jo, S. Julia, "A System Design of Liquid Cooling Computer Based on the Micro Cooling Technology," Thermal and Thermomechanical Phenomena in Electronics Systems, ITHERM '06. May 30 - June 2 (2006) San Diego, CA, 157 - 160.

[8] Intel@ Pentium@ 4 Processor on 90 nm Process in the 775-Land LGA Package for Embedded Applications, Intel Corporation, November 2005.

[9] M. Iyengar, S. Garimella, "Design and Optimization of Microchannel Cooling Systems," Proc ITherm, May 2006, 54-62].

[10] R. Kempers, P. Kolodner, A. Lyons, A.J. Robinson, (2009) "A High-Precision Apparatus for the Characterization of Thermal Interface Materials," Review of Scientific Instruments, 80, 095111.

[11] M. Fabbri and V.K. Dhir, Optimized heat transfer for high power electronic cooling using arrays of microjets, Journal of Heat Transfer 127 (2005) 760-769.

[12] N. Yonehara, I. Ito, Cooling characteristics of impinging multiple water jets on a horizontal plane, Technology Report Kyushu University 24 (1982) 267-281.

ACCEPTED MANUSCRIPT

[13] A.M. Kiper, Impinging water jet cooling of VLSI circuits, International Communications in Heat and Mass Transfer 11 (1984) 517-526.

[14] L.M. Jiji, Z. Dagan, Experimental investigation of single-phase multijet impingement cooling of an array of microelectronic heat sources, in: W. Aung (Ed), Cooling Technology for Electronic Equipment, Hemisphere Publishing Corporation, Washington, D.C., 1988, pp. 333-351.

[15] Y. Pan, B.W. Webb, Heat transfer characteristics of arrays of free-surface liquid jets, Journal of Heat Transfer, 117 (1995) 878-883

[16] D.J. Womac, F.P. Incopera, S. Ramadhyani, Correlating equations for impingement cooling of small heat sources with multiple circular liquid jets, Journal of Heat Transfer 116 (1994) 482-486.

[17] A.J. Robinson, E. Schnitzler, "An experimental investigation of free and submerged miniature liquid jet array impingement heat transfer," Exp. Thermal and Fluid Science*,* 32, (2007) 1-13.

[18] B. Whelan and A.J. Robinson, "Nozzle Geometry Effects in Liquid Jet Array Impingement*,"* Applied Thermal Engineering, 29 (11-12) (2009) 2211-2221.

[19] N. T. Obot and T. A. Trabold, "Impingemnt heat transfer within arrays of circular jets: Part 1 - Effects of minimum , intermediate and complete crossflow for small and large spacing," Journal of Heat Transfer, Transactions ASME, 109 (1987) 872-879, 1987.

[20] A.J. Robinson, "A Thermal-hydraulic Comparison of Liquid Microchannel and Impinging Liquid Jet array Heat Sinks for High Power Electronics Cooling," IEEE Transactions on Components and Packaging Technologies, 32 (2) (2009) 347- 357.

[21] F. P. Incropera and D. P. Dewitt, Introduction to Heat Transfer, 6th Edition. New York: John Wiley and Sons, Ch. 8, Pg. 43.

[22] W.A. Khan, J.R. Culham, and M.M. Yovanovich, "Analytical model for convection heat transfer from tube banks," Journal of Thermophysics and Heat Transfer, 20 (2006) 720-727.

ACCEPTED MANUSCRIPT

List of Figures

Figure 1: Complete heater block and housing assembly.

Figure 2: Schematic of jet impingement heat transfer apparatus.

Figure 3: a-c) Renderings of the jet impingement waterblock, d) photograph of jet impingement water block.

Figure 4: Remote heat exchanger, a) front view, b) rear view. Air is blown across the heat exchanger, not drawn through it.

Figure 5: Staggered tube bundle in cross flow.

Figure 6: R_{th} vs. $\dot{V}$ for MC-TDX and jets water block.

Figure 7: ΔP vs. $\dot{V}$ for MC-TDX and jets water block, Q=100W.

Figure 8: R_{th} vs. Q_{pump} for MC-TDX and jets water block, Q=100W.

Figure 9: R_{th} vs. Q for jets/tube system at $\dot{V} = 5.25$ L/min.

Figure 10: Variation of the water inlet, waterblock base and the heater block surface temperature with imposed power.

Figure 11: R_{th} vs. $\dot{V}$ for the jets/tubes system at Q = 75 W.

Figure 12: (a) Q_{pump} vs. $\dot{V}$ (b) R_{th} vs. Q_{pump} for the jets/tubes system at Q = 75 W.

ACCEPTED MANUSCRIPT

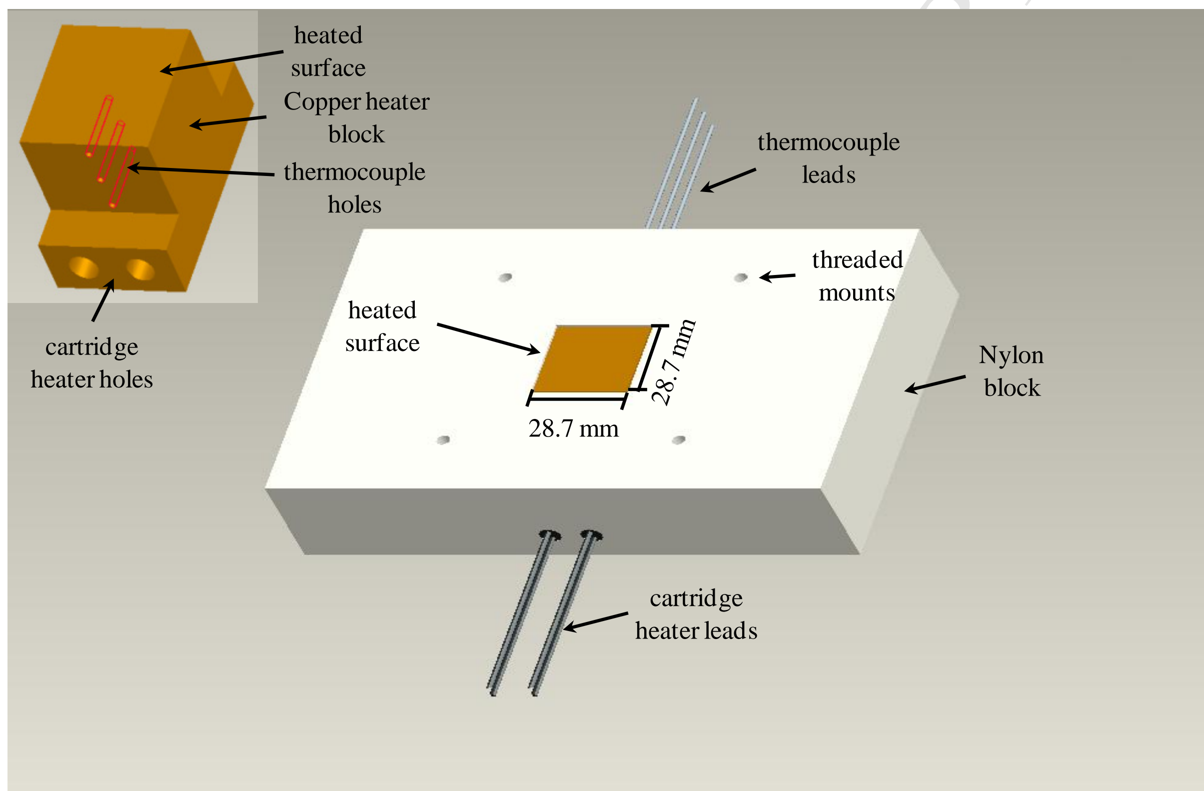
heated
surface
Copper heater
block
thermocouple
holes
cartridge
heater holes
thermocouple
leads
threaded
mounts
heated
surface
28.7 mm
28.7 mm
Nylon
block
cartridge
heater leads

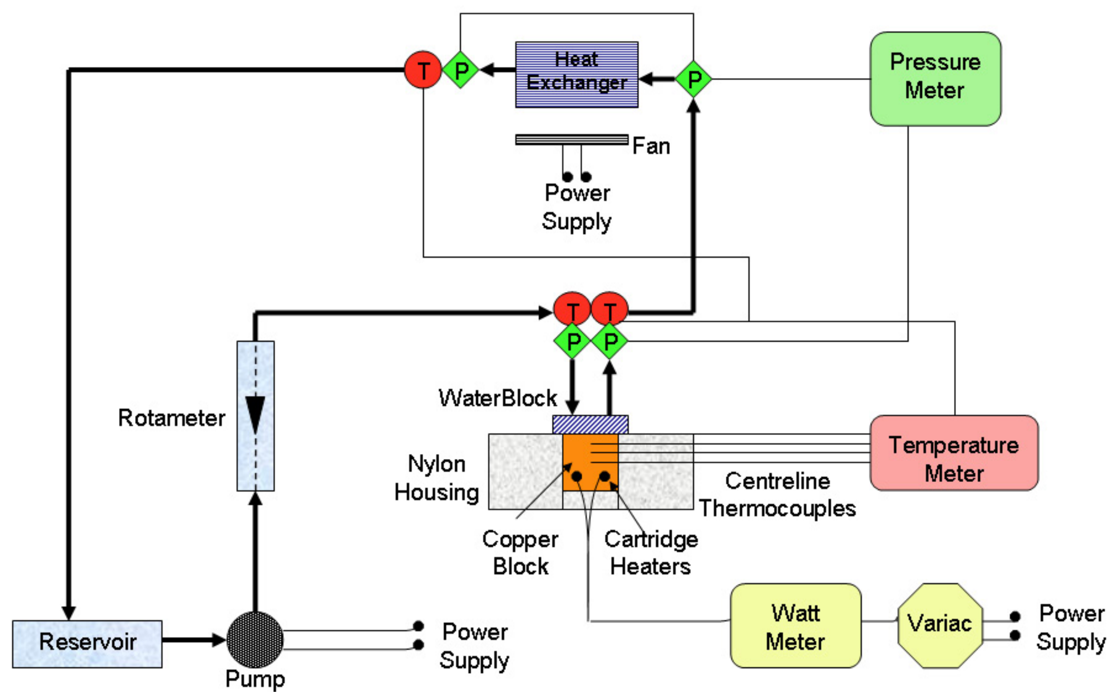

ACCEPTED MANUSCRIPT

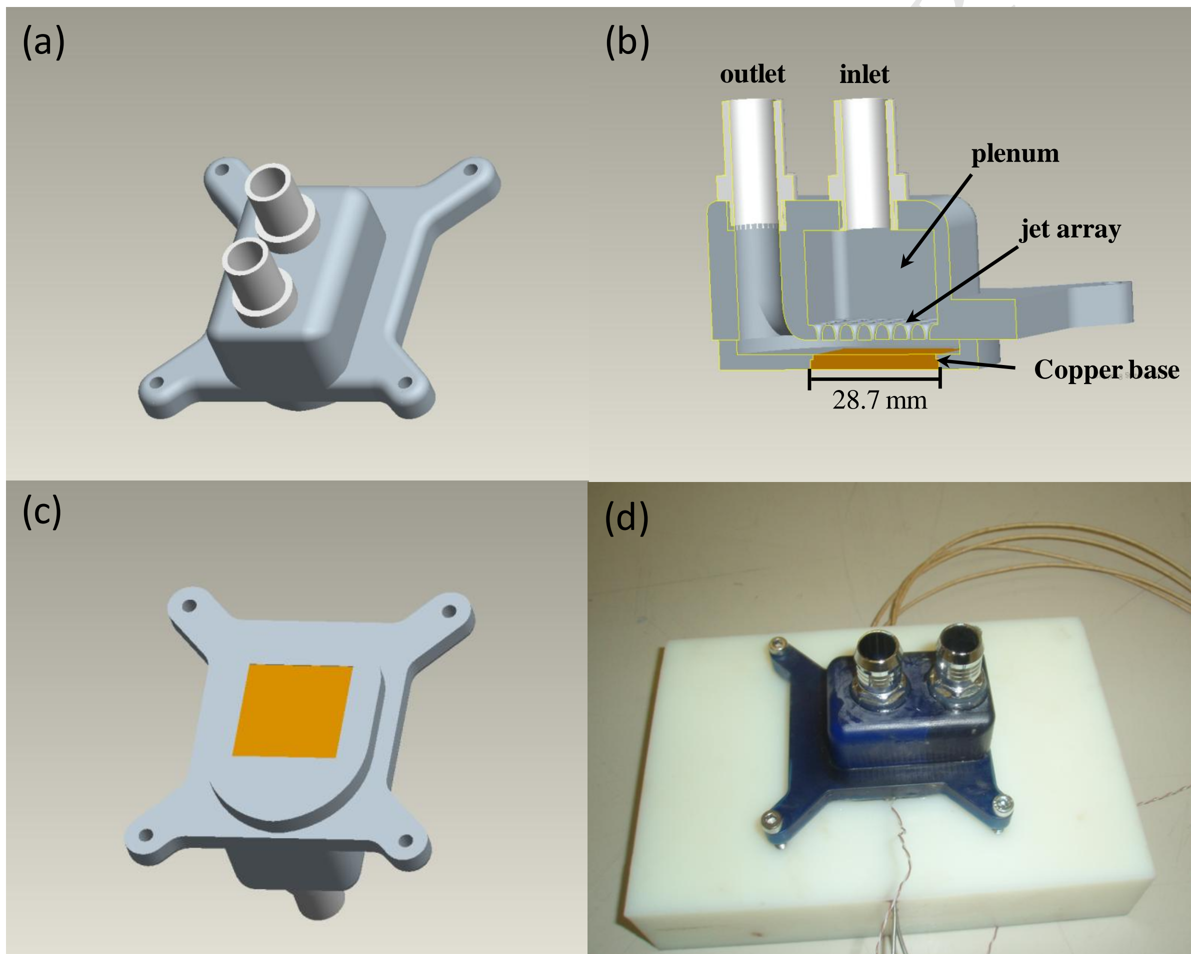

ACCEPTED MANUSCRIPT

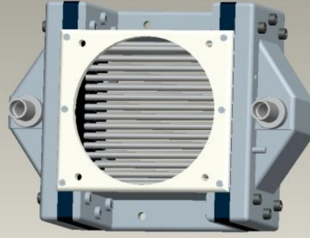

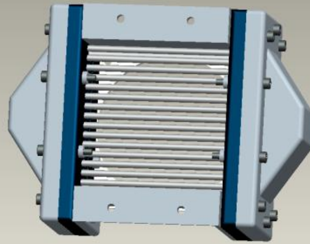

ACCEPTED MANUSCRIPT

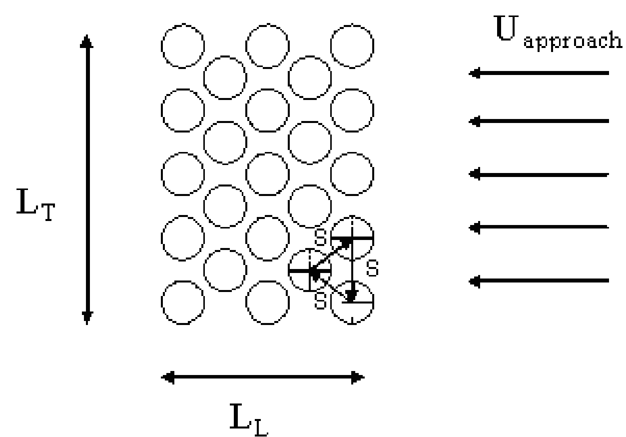

ACCEPTED MANUSCRIPT

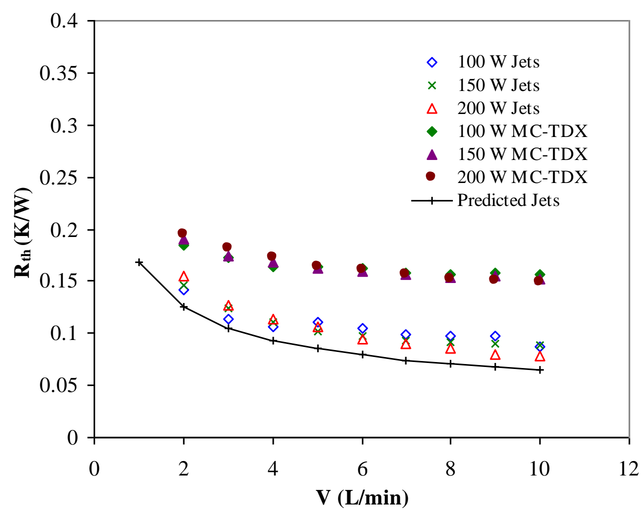

ACCEPTED MANUSCRIPT

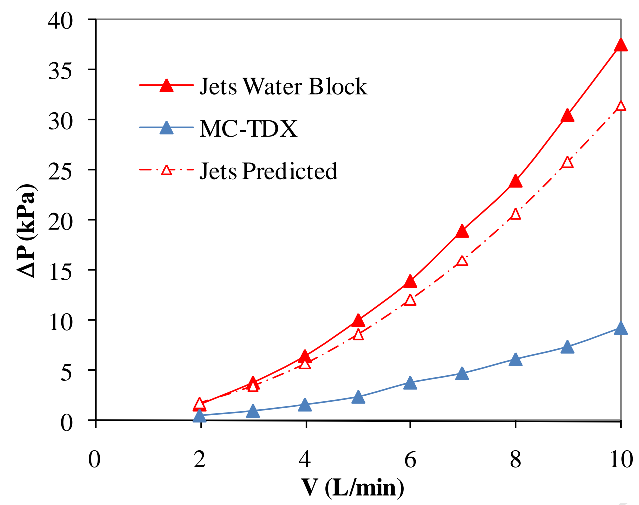

ACCEPTED MANUSCRIPT

ACCEPTED MANUSCRIPT

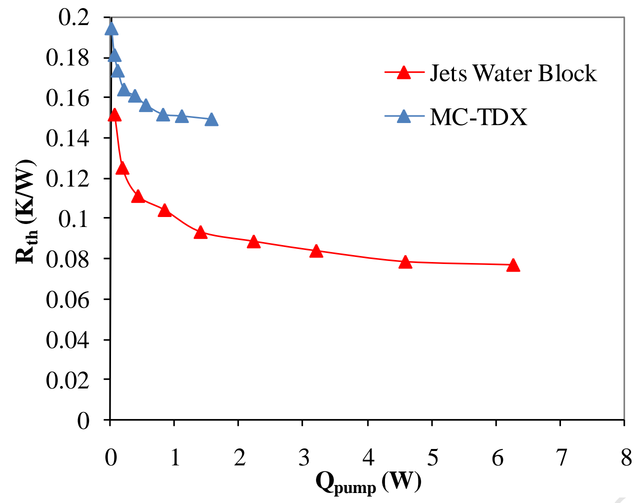

ACCEPTED MANUSCRIPT

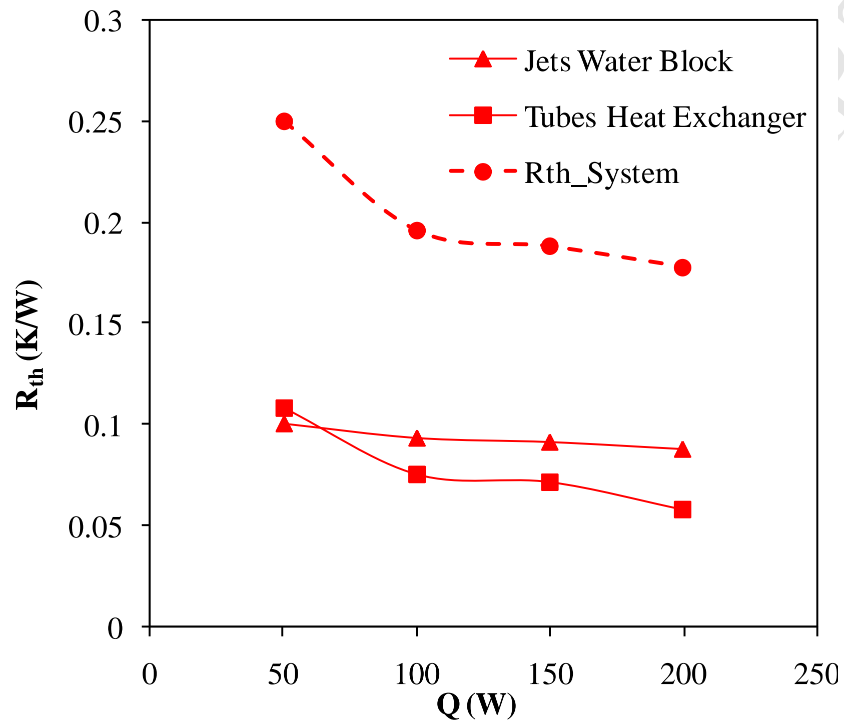

ACCEPTED MANUSCRIPT

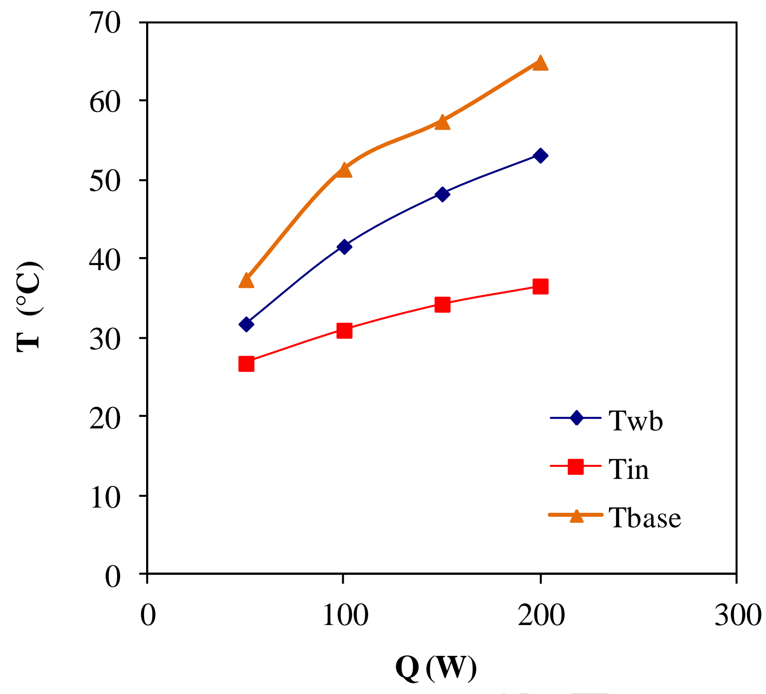

ACCEPTED MANUSCRIPT

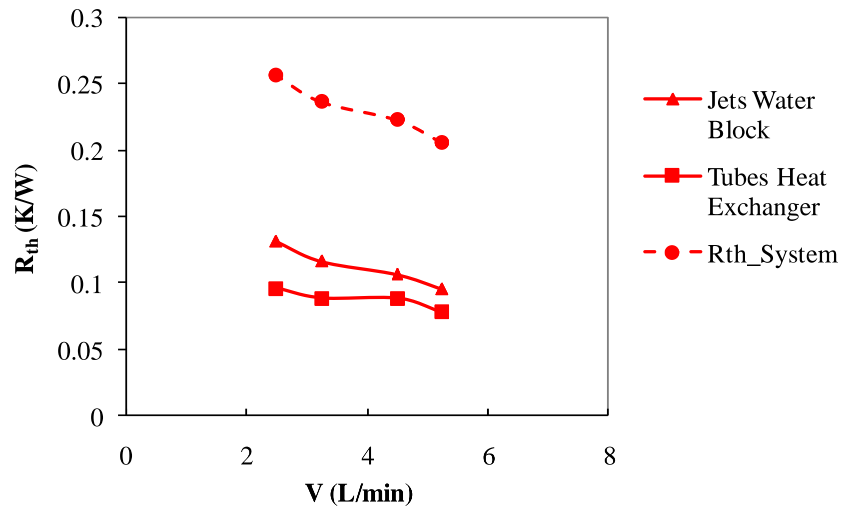

ACCEPTED MANUSCRIPT

ACCEPTED MANUSCRIPT

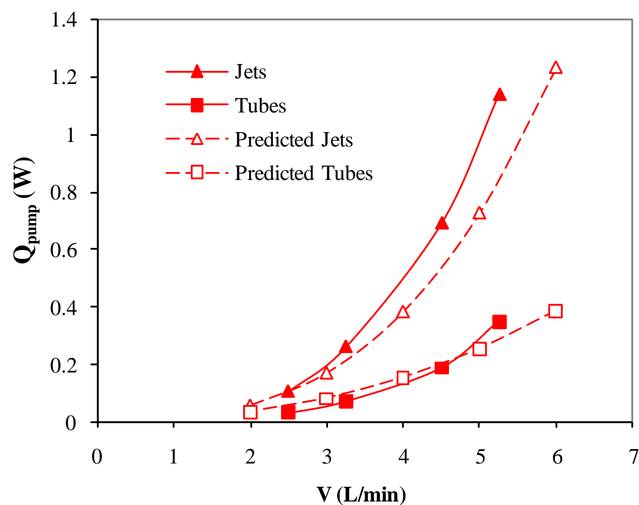

(a)

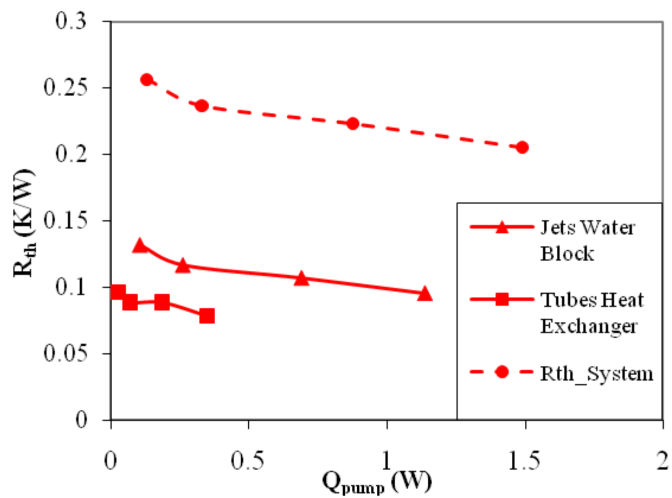

(b)

ACCEPTED MANUSCRIPT

Highlights

- We describe a liquid CPU cooling system.
- The cooling capacity is 200 W for a surface area of 8.24 cm^2.
- The overall thermal resistance is 0.18 K/W.
- The system requires approximately 1.5 W of hydraulic power.
- The system is amenable to low cost manufacturing

ACCEPTED MANUSCRIPT